

Apparent non-statistical binding in a ditopic receptor for guanosine†

Asawin Likhitsup,^a Robert J. Deeth,^a Sijbren Otto^b and Andrew Marsh^{*a}

Received 28th July 2008, Accepted 23rd January 2009

First published as an Advance Article on the web 24th March 2009

DOI: 10.1039/b812969j

Analysis of stepwise association constants for guests binding to more than one site in a receptor is expected to give a ratio of the first association constant to the second of about 4 : 1 on statistical grounds (since a second guest should have an equal chance of binding to a different site on the same, or a new molecule). Taking account of self-association in our analysis of a system in which the binding sites are close together, we observe a ratio closer to 1 : 1, indicative of non-statistical, or cooperative binding. The longer homologue built around two alkynes displays a very different ratio of stepwise association constants of about 7 : 1. We discuss the origins of this unusual behaviour in terms of steric interactions within the receptors and their corresponding complexes with guanosine derivatives.

Introduction

Quantitation of the interaction of guest molecules with receptors bearing multiple binding sites is of significance across supramolecular chemistry, structural biology, pharmacology of biological receptors and materials science.¹ Elucidating mechanistic pathways of association,^{2–5} including whether or not they take place with what is referred to as ‘cooperativity’,^{6–8} is thus of practical importance. We report here the binding studies of ditopic receptors for guanosine and the observation of what appears as a non-statistical,⁹ or cooperative binding event. The C_2 -symmetric ditopic receptors are composed of two cytidine moieties¹⁰ linked through either an alkyne **1**, or dialkyne **2** at C5 (Fig. 1) as reported previously.¹¹ Job’s plot revealed a 1 : 2 stoichiometry of binding between **1** or **2** with **3** and the association constants were reported in deuteriochloroform as 2670 and 2200 M^{-2} , respectively, using a naïve 1 : 2 binding model. We move herein towards a more

complete analysis of the equilibria involved, whilst recognising the limitations of the methods employed. Receptors with more than one mode of association present real challenges in terms of experimental design, data acquisition and the mathematical algorithms required to unambiguously assign association constants, particularly of relatively weakly interacting supramolecular assemblies.^{12,13}

Curve fitting methods

NMR titration is an accessible and informative method used in determining association constants between both small and large molecules in solution.^{14–17} Titration data may be analysed by: (i) graphical methods such as the Benesi–Hildebrand (double reciprocal) plot and Scatchard plot; or (ii) direct curve fitting methods. Curve fitting methods require no approximations and allow almost unrestricted distribution of experimental points (host and guest concentrations), within usual limitations.^{17,18} For example, the Saunders–Hyne method¹⁹ (two-state approximation) has been used to determine the strength of hydrogen bonded aggregates.²⁰ A number of computer programs have been created for curve fitting; however, those more commonly available are limited to 1 : 1, 1 : 2 or 2 : 1 complexes.¹⁵ Several commercial programs (including Specfit/32TM,²¹ HypNMR,²² Dynafit²³ and Prism²⁴) and non-commercial algorithms (EQNMR,^{25,26} NMRTit,²⁷ HOSTEST²⁸ and ASSOCIATE as recently implemented²⁹) allow more sophisticated models to be used, although each has limitations. In more complex cases, numerical methods are the best solution because of the number of parameters involved. Recently, a complete treatment that allows complex two component systems of the type studied herein to be tackled has been disclosed, and its eventual application to this system will no doubt be revealing.¹³

In the case of 1 : 1 complexes, curve fitting is usually straightforward.³⁰ When a 1 : 2, 2 : 1 complex, or multiple equilibria are present, finding the mathematical solution for curve fitting becomes progressively more problematic and some results using this approach have been found to be less satisfactory by some authors.^{31–33} In the case of weak 1 : 2 complexes with $K_1 < < K_2$,

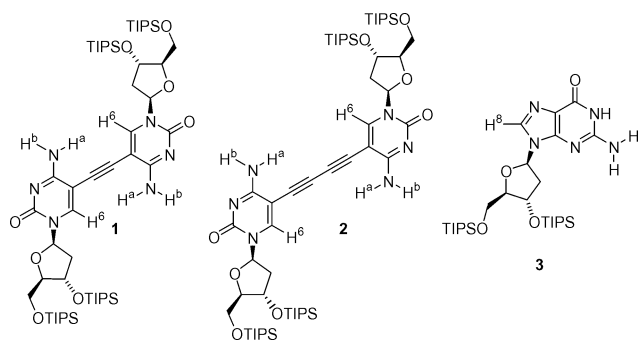


Fig. 1 Receptors **1**, **2** and guanosine derivative **3** used for binding studies; TIPS = triisopropylsilyl.

^aDepartment of Chemistry, University of Warwick, Coventry, United Kingdom CV4 7AL. E-mail: a.marsh@warwick.ac.uk

^bCentre for Systems Chemistry, University of Groningen, Nijenborgh 4, 9747 AG, Groningen, The Netherlands. E-mail: s.otto@rug.nl

† Electronic supplementary information (ESI) available: Data for dimerisation of **1** and **2**, self-association of guanosine **3** and binding between receptors **1** and **2** and guanosine **3**. See DOI: 10.1039/b812969j

it has been shown that the determination of the stepwise binding constants is not possible.³¹

Results and discussion

Self-association of receptors **1** and **2**

Previous studies on a lipophilic cytidine derivative have revealed weak self-association with a dimerisation constant of 30–40 M⁻¹,^{34,35} also observed in a portion of the crystal structure of **2** (Fig. 2).¹¹ Thus, we set out to re-evaluate the self-association of **1** and **2** using ¹H NMR dilution¹⁴ in the first instance. Expecting a relatively weak association constant, we chose an initial concentration of about 0.01 M in deuteriochloroform, meeting usual criteria for its accurate determination,^{16,17} *i.e.* that $\frac{1}{10} \cdot \frac{1}{K_a} \leq [G]_i \leq 10 \cdot \frac{1}{K_a}$ where K_a is the expected association constant and $[G]_i$ is the total concentration of guest to be diluted.

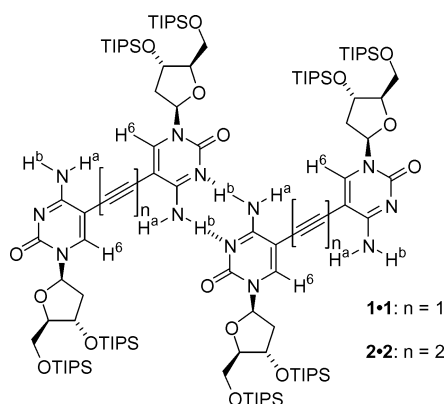


Fig. 2 Dimers of **1** and **2**, 1•1 and 2•2; respectively.

The ¹H NMR spectra of **1** and **2** in deuteriochloroform are very similar, but in **1** H-6 appears at 8.14 ppm, whilst for **2** H-6 appears at 8.22 ppm. The two exocyclic NH₂ protons are non-equivalent with NH^a appearing at higher field than H^b: 5.6–5.9 and

5.6–6.0 ppm for **1** and **2** respectively, in agreement with previous observations.³⁴

The dimerisation of **2** was initially studied by monitoring the NMR chemical shifts of NH^a, NH^b and H-6 upon dilution (tabulated in ESI Part 2†). Except for the first data point the concentration of the receptor was calculated using tetramethylsilane as an internal standard. This complete data set was fitted using the Saunders–Hyne model,^{14,15} assuming that only two major components (monomer and dimer) are significant in the equilibrium,¹⁹ resulting in the curves shown in Fig. 3 giving the best dimerisation constant, $K_{2,2}$ as 340 ± 7 M⁻¹ in deuteriochloroform. Errors were estimated by adapting a least-squares method^{36,37} whereby data points in the spreadsheet are sequentially deleted and a new least-squares fit carried out to estimate the association constant lacking that data point. The complete data set could not be fitted at all to either a trimer model (data not shown), or a ‘dimer of dimers’ model (*cf.* self-association of guanosine **3**). Further confidence in the quality of the dataset and fitting comes from evaluation of the probability of binding,¹⁷ $p = 2 \times \frac{[2 \cdot 2]}{[2]_{tot}}$, found to be $0.37 < p_2(2 \cdot 2) < 0.82$ over the titration interval (see ESI Part 2†). The best quality data and fitting is found for $0.20 < p < 0.80$, although data outside this range is still useful if errors therein can be fully described.

One limitation of the model used is that it cannot distinguish dimerisation from isodesmic polymeric association.^{12,38} In order to do this, an independent method such as VPO,¹² other methods for estimating M_n or M_w , or more sophisticated numerical approaches¹³ are required. The same dilution process was also studied by isothermal titration calorimetry (ITC; see ESI Part 1†) and fitted using a dimerisation model to give an association constant $K_{2,2} = 90$ M⁻¹ which is noticeably different, although much closer to $K_{1,1}$ observed for the shorter receptor **1**.

Minor conformational change of **2** upon dimerisation results in shielding of H-6 and deshielding of NH^a. Upon dilution, the signal for H-6 shifted downfield ($\Delta\delta = 0.08$ ppm) whilst that for NH^a moved upfield ($\Delta\delta = 0.37$ ppm). The effect of the alkyne is

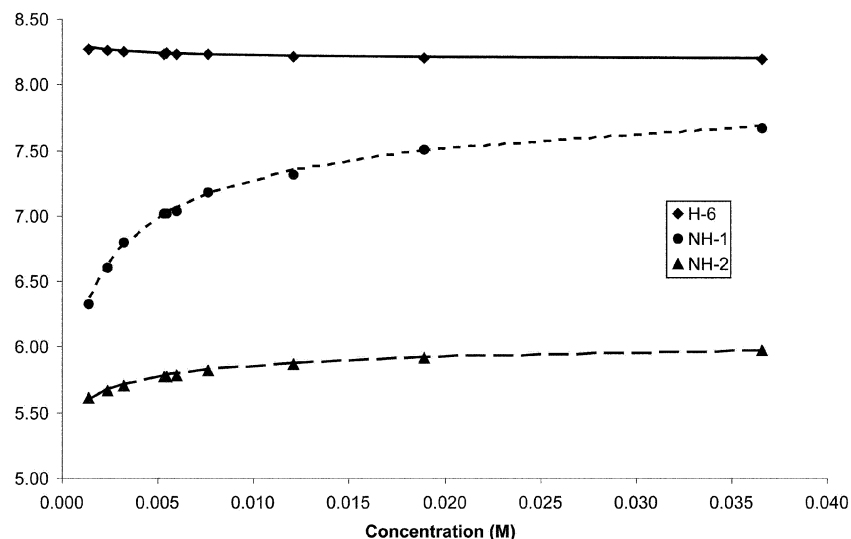


Fig. 3 Curve fitting from NMR dilution of **2**; $K_{2,2} = 340 \pm 7$ M⁻¹.

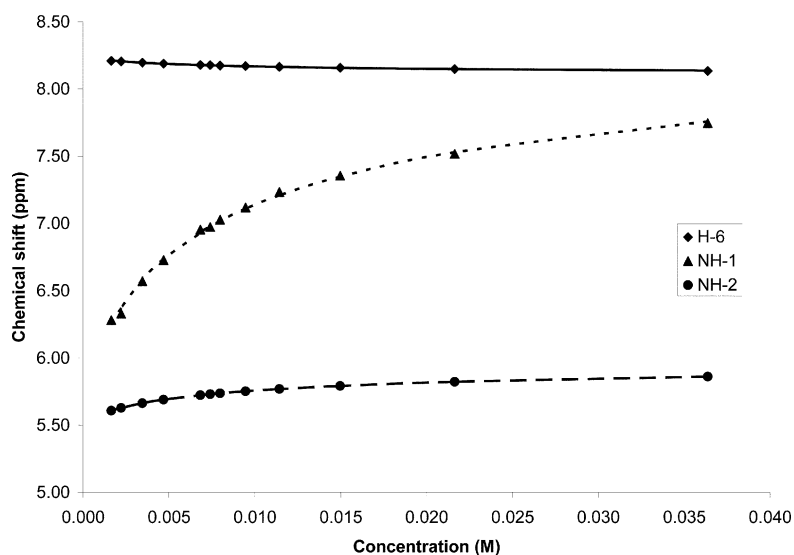


Fig. 4 Curve fitting from NMR dilution of **1** in CDCl_3 ; $K_{1,1} = 83 \pm 3 \text{ M}^{-1}$.

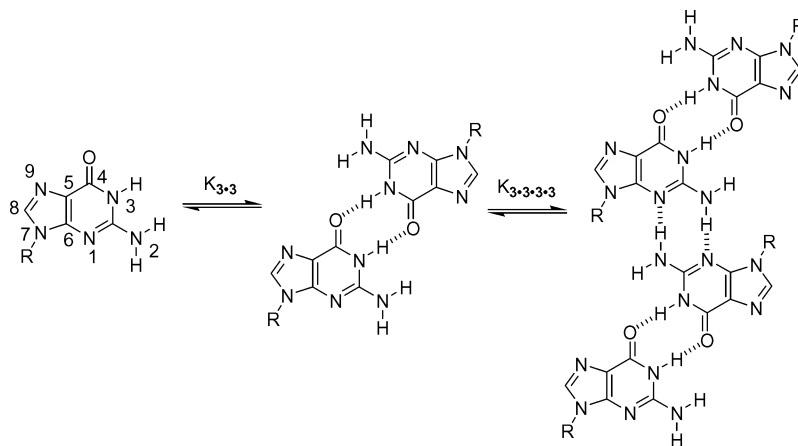


Fig. 5 Self-association model of lipophilic guanosine **3** in chloroform.

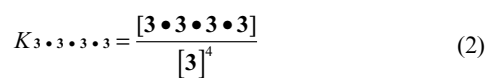
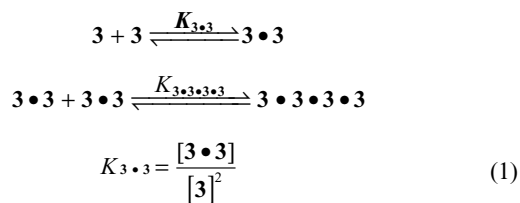
more pronounced in NH^a due to greater proximity of the alkyne π -orbital compared to H-6. Although the NMR titration result agrees with the dimerisation model, receptor **2** may also form a hydrogen bonded tape at higher concentration, observed as a viscous gel in chloroform, leading ultimately to the solid state structure reported previously.¹¹ The only significant difference in the ^1H NMR spectra of **1** and **2** is that H-6 of **1** appears at higher field. Upon dilution, all three protons are shifted in the same way as in **2**: H-6 downfield, NH^a upfield and NH^b upfield (Fig. 4). Again, conformational changes may be used to explain the peak shifts of H-6 and NH^a .

Treatment of the NMR shift data from the dilution of monoalkyne **1** by simultaneous curve fitting of H-6, NH^a and NH^b revealed $K_{1,1} = 83 \pm 3 \text{ M}^{-1}$ in deuteriochloroform. The probability of binding for the receptor **1** in the dimer, $p_1(\mathbf{1}\cdot\mathbf{1})$ was found to be $0.18 < p_1(\mathbf{1}\cdot\mathbf{1}) < 0.67$ over the titration interval. The association constants for lipophilic cytidines have been consistently reported to be around $30\text{--}40 \text{ M}^{-1}$.^{35,39} Since there are two cytidines in each receptor, the dimerisation constant of $83 \pm 3 \text{ M}^{-1}$ for **1** is consistent with the reported values, although it contrasts with the higher value of $340 \pm 7 \text{ M}^{-1}$ found for dialkyne **2**.

Self-association of guanosine derivative **3**

The structure of lipophilic guanosine in chloroform has been extensively studied by Gottarelli and co-workers.⁴⁰⁻⁴² It has been shown that **3** readily dimerises through hydrogen bonding between N3-H and O4 (Fig. 5). At high concentration, the weaker hydrogen bonds between N1 and N2-H connect the dimers together to form guanosine ribbons (in the absence of metal ions) resulting in the observation of viscous gels.⁴²

In order to devise a model for curve fitting, the following equilibria are considered:



Mass balance:

$$[3]_0 = [3] + 2 \times [3 \bullet 3] + 4 \times [3 \bullet 3 \bullet 3 \bullet 3] \quad (3)$$

Chemical shift:

$$\delta_{\text{cal}} = \chi_3 \delta_3 + \chi_{3 \bullet 3} \delta_{3 \bullet 3} + \chi_{3 \bullet 3 \bullet 3 \bullet 3} \delta_{3 \bullet 3 \bullet 3 \bullet 3} \quad (4)$$

Rearrangement and substitution of (1) and (2) into (3) gives a polynomial equation. If curve-fitting is performed using the solution of this equation, problems arise in selecting the correct non-imaginary root.⁴³ This method is inflexible and time-consuming because the mathematical solution for the polynomial must be derived for each system. It is therefore not surprising that most curve-fitting programs only extend to 1 : 2 binding.^{15,16,44}

In order to address this problem, a more flexible curve-fitting routine was devised based on NMR chemical shift simulation using numerical methods in MS Excel[®].³⁶ The method, as described by Wilcox and co-workers, has been employed in the study of ternary systems.⁴⁵ This routine requires an input of $K_{3 \bullet 3}$ and $K_{3 \bullet 3 \bullet 3 \bullet 3}$, with a known initial concentration $[3]_0$; there is only one set of $[3]$, $[3 \bullet 3]$, and $[3 \bullet 3 \bullet 3 \bullet 3]$ that satisfies eqn (1), (2) and (3).

Using this template, the ‘Solver’ function in Microsoft Excel[®] was used to find the value of $[3]$ at each concentration with the input K values (see Experimental for details). We then calculated δ_{cal} from the input δ_3 , $\delta_{3 \bullet 3}$ and $\delta_{3 \bullet 3 \bullet 3 \bullet 3}$, parameters that were readily easily estimated from the titration curve. Non-linear least squares curve fitting was then performed by varying δ_3 , $\delta_{3 \bullet 3}$ and $\delta_{3 \bullet 3 \bullet 3 \bullet 3}$ to give the best fit between δ_{cal} and δ_{obs} . The association constants $K_{3 \bullet 3}$ and $K_{3 \bullet 3 \bullet 3 \bullet 3}$ were iterated manually and the pair that gave the smallest sum of chi squared (S) values from curve fitting was chosen. Errors were again estimated by the same adapted least-squares method as previously.^{36,37} The algorithm was benchmarked against recent literature data⁴⁶ where the challenge of 2 : 1 binding was faced using a modified commercial HypNMR package,²⁶ underlining the non-standard nature of the task (see ESI Part 1†). The new spreadsheet was able to replicate the observed equilibrium constants in that 2 : 1 system satisfactorily.

The NMR spectrum of **3** shows only two sets of amine signals. Unlike the NH_2 in cytidine, the guanosine NH_2 rotates quickly on the NMR timescale and the two exocyclic NHs are magnetically equivalent.³⁴ Upon dilution, the N3–H shifts downfield from 11.99 to 12.08 ppm. Similarly, H-8 shifts downfield from 7.76 to 7.81 ppm. Analogously, NH_2 shifts upfield from 6.25 to 5.90 ppm (Fig. 6). Since the induced chemical shifts for H-8 and NH_2 are relatively small, curve fitting based on these shifts alone might give rise to a higher systematic error than the current procedure, fitting all the limiting chemical shifts for H-8, NH_2 and N3–H in a single step to minimize the combined S values. The two association constants were then carefully iterated to find the best solutions, with an error limit representing the standard deviation of least-squares fits lacking sequential data points as above. The resulting association constants in deuteriochloroform, $K_{3 \bullet 3}$ and $K_{3 \bullet 3 \bullet 3 \bullet 3}$ are found to be 370 ± 72 and $15 \pm 1 \text{ M}^{-1}$ respectively, in agreement with a previous report ($K_{\text{dimer}} 300 \text{ M}^{-1}$), although higher order aggregates were not considered in that analysis.³⁵ The probability of binding for significant aggregated species over the titration interval was found to be $0.53 < p_3(\mathbf{3 \bullet 3}) < 0.66$ and $0.015 < p_3(\mathbf{3 \bullet 3 \bullet 3 \bullet 3}) < 0.31$ respectively.

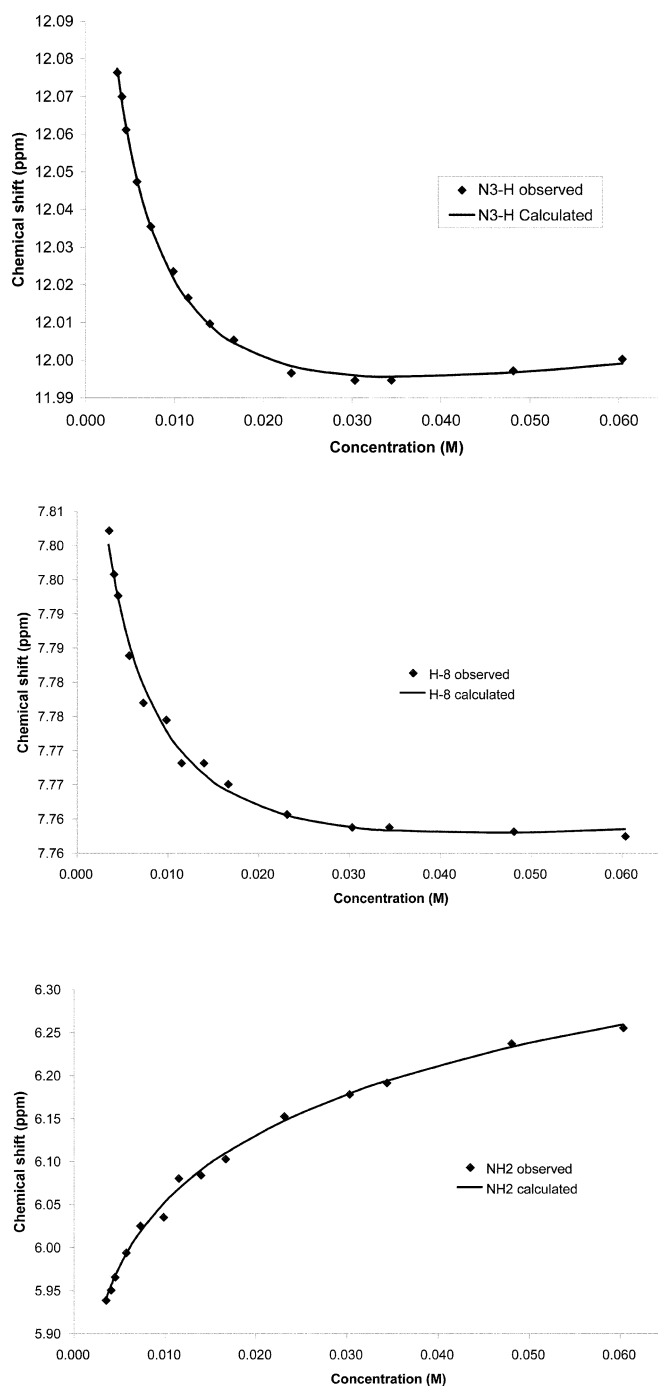


Fig. 6 Curve fitting for NMR dilution of **3** in CDCl_3 . The three titration curves (A) N3–H (B) H-8 and (C) NH_2 are fitted simultaneously to give $K_{3 \bullet 3}$ of 370 ± 72 and $K_{3 \bullet 3 \bullet 3 \bullet 3}$ of $15 \pm 1 \text{ M}^{-1}$.

Preliminary ITC results are inconclusive since the data could not be fitted properly to a calculated curve using the above ‘dimer of dimers’ model, although this may be due to the way data is treated following standard ITC experiments (see ESI Part 1†).

Binding studies of receptors **1** and **2** with guest **3**

Binding studies between receptor **2** and guest **3** (Fig. 7) were carried out by NMR titration in CDCl_3 . The input for the freely

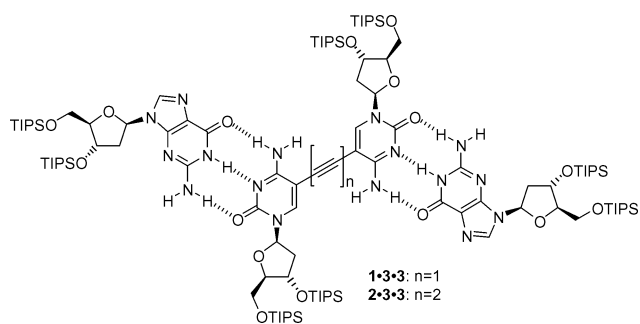


Fig. 7 Complexation of receptors **1** or **2** with **3**; TIPS = triisopropylsilyl.

available NMRtit program²⁷ requires that the concentration of the host **2** is held constant throughout the experiment. In the first attempt, the titrant **3** was dissolved with host **2** stock solution, as required, but the concentration of **2** was now so low that it was impossible to unambiguously follow the now broad N–H signals (chosen since they presented the greatest change in chemical shift) in the ¹H NMR spectrum. Thus, the titration was performed by adding a concentrated solution of **3** in small portions to a relatively concentrated solution (*ca.* 0.01 M) of **2** in the NMR tube, thereby allowing concentration of host **2** to change with each addition of guanosine **3**. It was recognised that data analysis would no longer be possible using, for example NMRtit, but one benefit is that binding of receptor to guest stays within the preferred 20–80% even when a 3-fold excess of guest has been added. This would be more difficult to achieve whilst maintaining practicable dynamic range in the NMR experiment if more host were added together with guest in order to maintain a constant host concentration. The NH^b in **2** was followed as it is directly involved in hydrogen bonding to the guest and the induced chemical shift change is quite large. The initial data point now overlapped with that for the experiment to determine host dimerization, [HG] = 0 (see ESI Part 2†), adding confidence to the data fitting. All concentration changes were calibrated using the aromatic peak

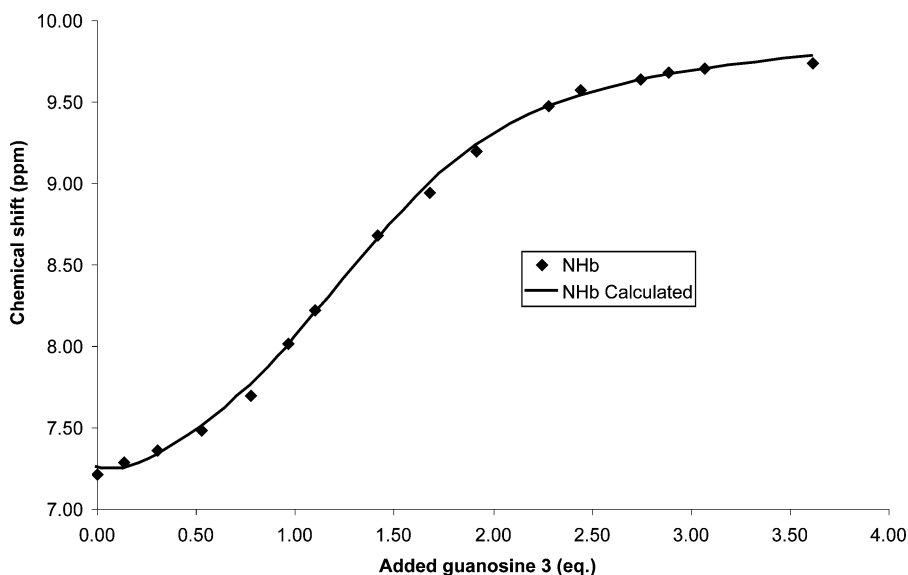
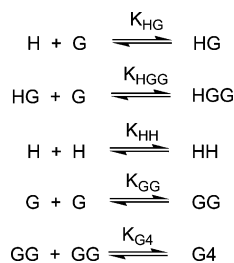


Fig. 8 Curve fitting of NMR titration in CDCl₃ between **2** and **3**. $K_{2,3}$ 8100 ± 380; $K_{2,3,3}$ 1170 ± 80 M⁻¹.

areas (H-6 for **2** and H-8 for **3**) against TMS as an internal standard.

The equilibria considered are shown in Scheme 1 (*H* = host, *G* = guest).



Scheme 1 Equilibria in the binding studies between **2** and **3**.

And following the standard Saunders–Hyne model; association constants are:

$$K_{\text{HG}} = \frac{[\text{HG}]}{[\text{H}][\text{G}]} \quad (5)$$

$$K_{\text{HGG}} = \frac{[\text{HGG}]}{[\text{H}][\text{HG}]} \quad (6)$$

Mass balance for both host and guest is

$$[\text{H}]_0 = [\text{H}] + 2[\text{HH}] + [\text{HG}] + [\text{HGG}] \quad (7)$$

$$[\text{G}]_0 = [\text{G}] + 2[\text{GG}] + 4[\text{G4}] + [\text{HG}] + 2[\text{HGG}] \quad (8)$$

The chemical shift was calculated from the contribution of all the species present in the equilibrium according to Scheme 1:

$$\delta_{\text{cal}} = \chi_{\text{H}}\delta_{\text{H}} + \chi_{\text{HH}}\delta_{\text{HH}} + \chi_{\text{HG}}\delta_{\text{HG}} + \chi_{\text{HGG}}\delta_{\text{HGG}} \quad (9)$$

The limiting chemical shift of host dimer **2·2** as well as the self-association constants for both **2** and **3** were taken from NMR dilution studies described above. Upon addition of guest **3**, NH^b of **2** shifted downfield from 7.2 to 9.8 ppm. From the curve fitting (Fig. 8), the stepwise association constants are found as

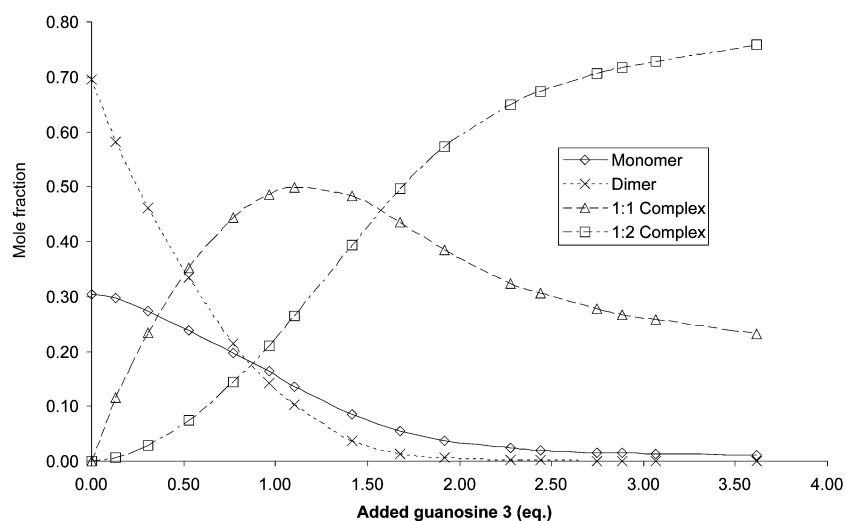


Fig. 9 Speciation curve for receptor **2** upon addition of **3** in CDCl_3 , showing monomeric **2**, dimeric **2**, 1 : 1 complex (**2-3**) and 1 : 2 complex (**2-3-3**).

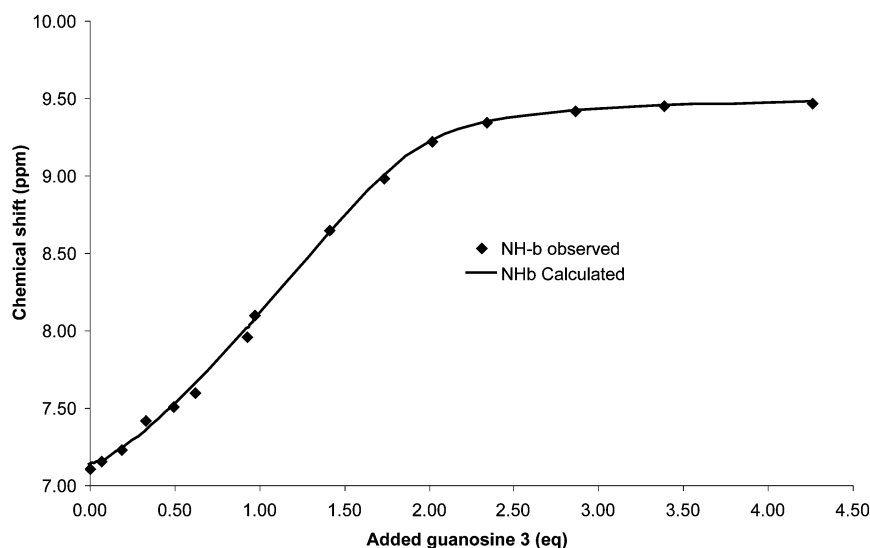


Fig. 10 Curve fitting of NMR titration in CDCl_3 between **1** and **3**. $K_{1,3} = 5180 \pm 210$, $K_{1,3,3} = 4800 \pm 170 \text{ M}^{-1}$.

$K_{2,3} = 8100 \pm 380$, $K_{3,2,3} = 1170 \pm 80 \text{ M}^{-1}$ in deuteriochloroform. Hence the overall microscopic association constant $K_a = K_{\text{HG}}K_{\text{HGG}}$ from NMR titration is $9.56 \times 10^6 \text{ M}^{-2}$. The probability of binding of **3** in forming the termolecular complex is described by $0.10 < p_3$ (**3-2-3**) < 0.60 over the titration interval. A speciation curve for **2** upon addition of **3** is shown in Fig. 9 and corresponding graphical probability of binding data is given in ESI Part 2.†

The NMR titration between **1** and **3** and subsequent curve fitting was performed by the same method (Fig. 10) whereby stepwise association constants were found to be $K_{1,3} = 5180 \pm 210$ and $K_{3,1,3} = 4800 \pm 170 \text{ M}^{-1}$ in deuteriochloroform. Hence the overall microscopic association constant $K_a = K_{\text{HG}}K_{\text{HGG}}$ from NMR titration is $24.86 \times 10^6 \text{ M}^{-2}$. The probability of binding of **3** in forming the termolecular complex is described by $0.14 < p_3$ (**3-1-3**) < 0.77 over the titration interval. A speciation curve for **1**

upon addition of **3** is shown in Fig. 11 and graphical fraction of guest in bound complex (probability of binding) data is presented in ESI Part 2.†

Previous studies on the G-C base pair in chloroform solution have revealed consistent association constants of $1.6\text{--}1.7 \times 10^4 \text{ M}^{-1}$.³⁹ Other systems containing DDA·AAD hydrogen bonding complexes show association constants *ca.* $1 \times 10^4 \text{ M}^{-1}$.⁴⁷ The stepwise binding constants found here by NMR between **1** and **2** with **3** are somewhat less than these values.

The stepwise binding of receptors **1** and **2** with **3**, summarised in Fig. 12 and Fig. 13 respectively, differs significantly. According to Ercolani's assessment of cooperativity,⁶ the ratio between K_{HG} and K_{HGG} should be 4 : 1 for statistical, or non-cooperative interaction. Binding of just one equivalent of guest **3** to either C_2 -symmetric **1** or **2** is a symmetry breaking process, with an expected entropic

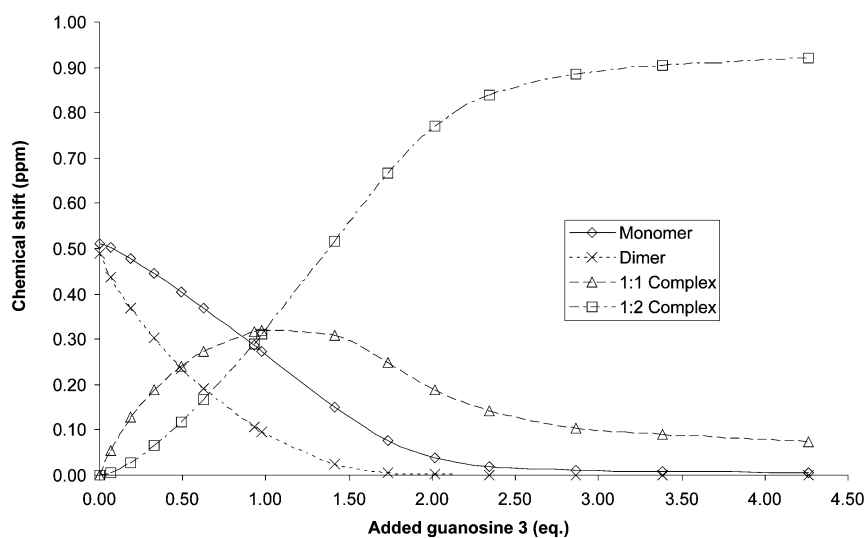


Fig. 11 Speciation curve for **1** upon addition of **3** in CDCl_3 .

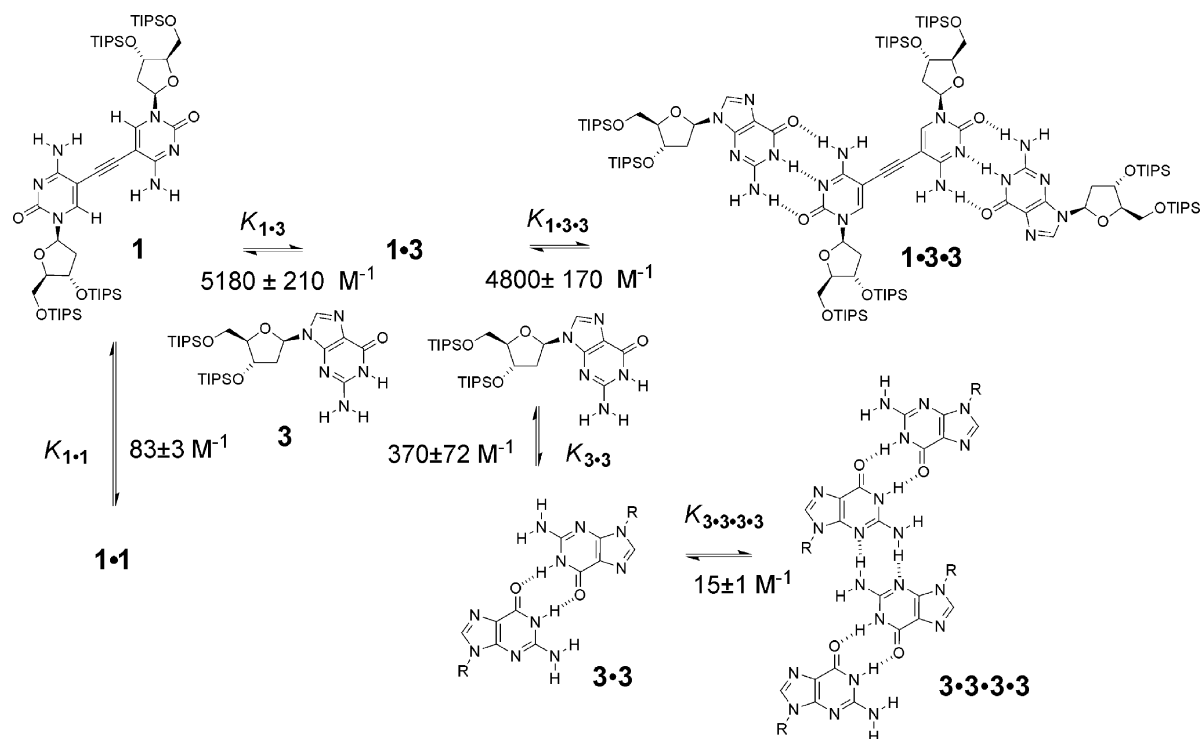


Fig. 12 Summary of equilibria in deuteriochloroform for monoalkyne receptor **1**.

cost. The second equivalent of **3** then has choice between binding to a new ditopic receptor molecule or the 1 : 1 complex, giving an apparent stepwise association complex.

Binding between **2** and **3** gave $K_{\text{HG}}/K_{\text{HGG}}$ of *ca.* 7 : 1, suggestive of close to independent, or possibly anti-cooperative, binding, that would be consistent with the statistically expected value (*ca.* 4 : 1). On the other hand, binding between **1** and **3** gave a $K_{\text{HG}}/K_{\text{HGG}}$ ratio close to 1, indicating that binding of the first ligand **3** is in some way beneficial to a subsequent binding event, *i.e.* positive cooperativity is observed. The origin

of this differing cooperativity must ultimately stem from the different structures of the receptors themselves. We observe from preliminary DFT calculations on simplified analogues of **1** and **2** lacking the ribose rings that rotation around the central alkyne bond alone has no significant energetic cost (data not shown). However, simple molecular model building of mono-alkyne host **1** using the Merck Molecular Mechanics Force Field (MMFF94x, well parameterised for dispersive interactions) with an implicit solvation model,⁴⁸ dielectric = 10, indicates that the four bulky triisopropylsilane protecting groups interact to a significant extent

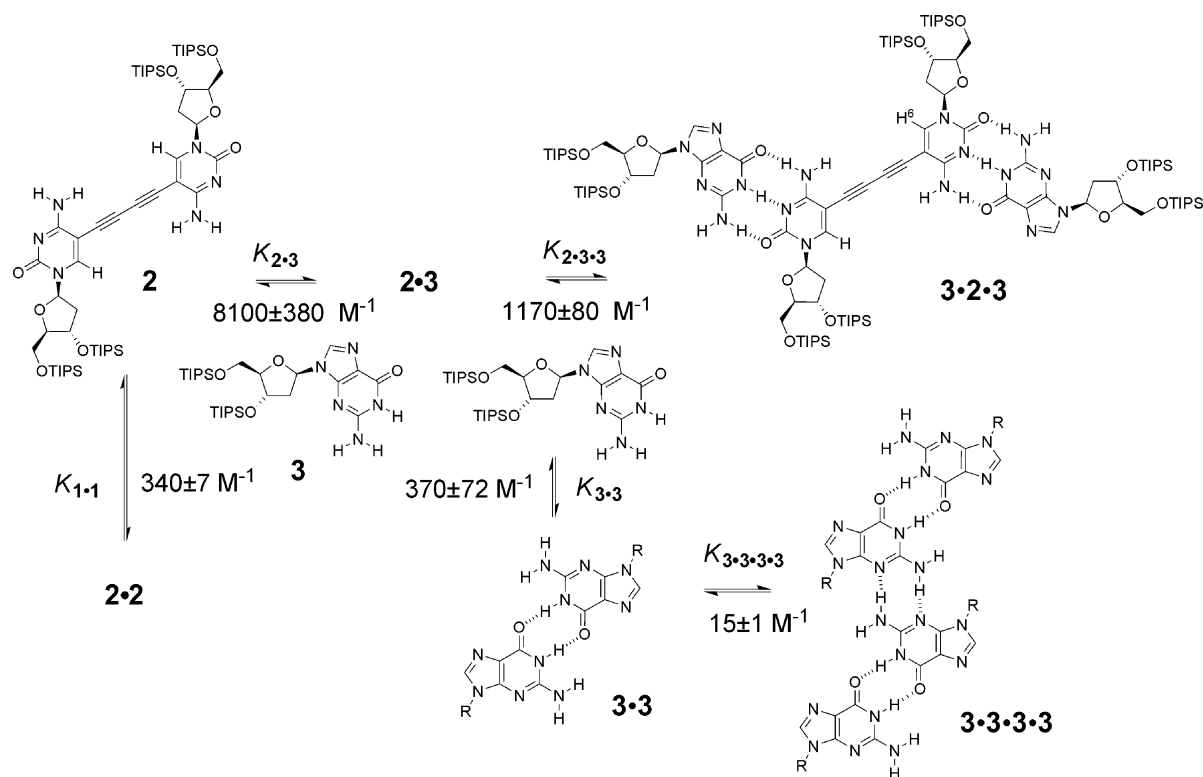


Fig. 13 Summary of equilibria in deuteriochloroform for dialkyne receptor **2**.

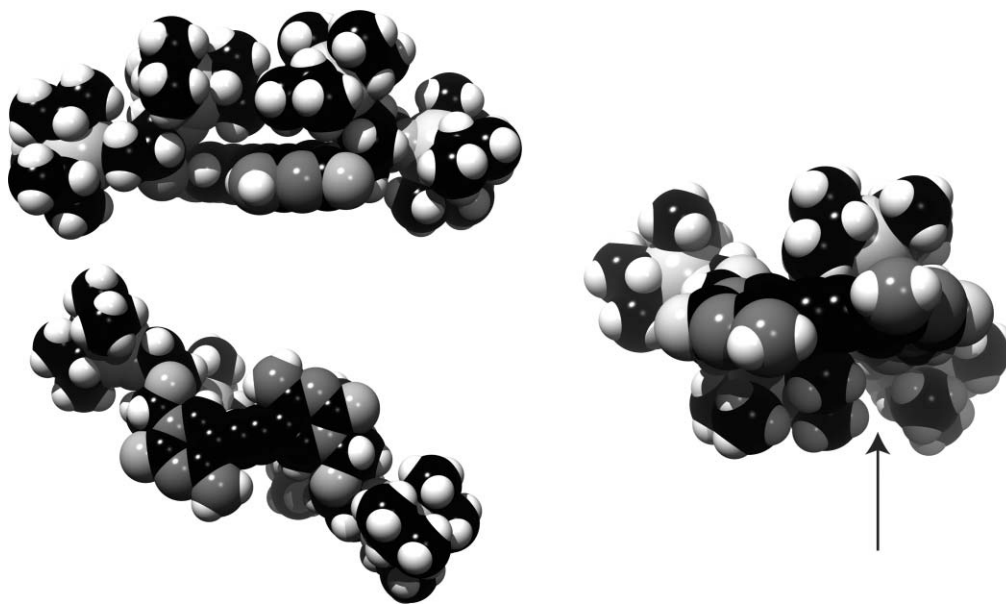


Fig. 14 C-P-K models of **1** at E_{\min} (left) dihedral $\approx 0^\circ$ side & plan views and E_{\max} (right) dihedral $\approx 165^\circ$ with interacting TIPS groups arrowed at rear of structure.

(Fig. 14), translating a rotational motion around the alkyne axis into a perpendicular geared, or propeller motion. Thus considering a dihedral angle between *ca.* 200–315° as an energetically neutral position (Fig. 15) a barrier of *ca.* 2 kcal mol⁻¹ is observed at 165°, with a local minimum at 180° and a global minimum

between 0–30°. At this point the ribose moieties and bulky TIPS groups are about as far apart as possible. In comparison, close to 165° the two amine groups bypass one another with an overall ‘gearing’ effect as the TIPS groups also move past each other requiring interacting solvent rearrangement and possibly bringing

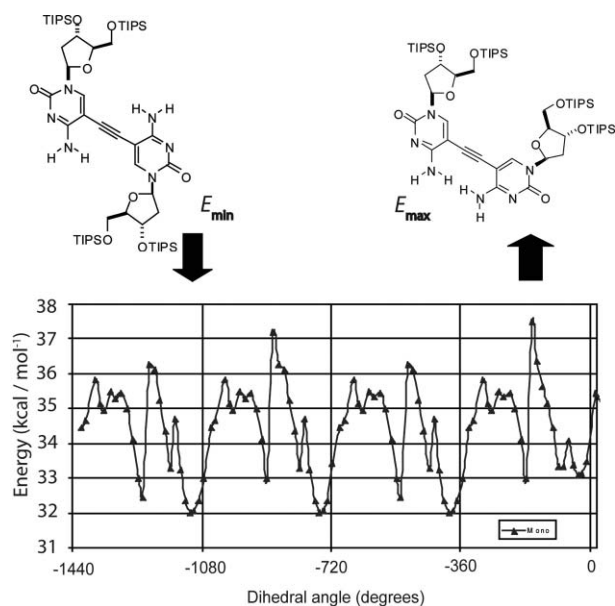


Fig. 15 Torsional energy vs. dihedral angle for monoalkyne **1**; E_{\min} at dihedral between $0\text{--}30^\circ$ and E_{\max} at ca. 165° .

enthalpic benefit due to dispersive forces once the steric barrier is overcome.

By contrast, rotation around the same dihedral in dialkyne receptor **2** shows an energy profile consistent with less repulsive interaction between the bulky TIPS groups with only 3 kcal mol⁻¹ difference between E_{\max} and E_{\min} , compared to an overall energy difference of 5.5 kcal mol⁻¹ for receptor **1** (Fig. 16). Whilst this data does not include the presence of a guanosine guest **3**, inspection of models such as Fig. 14 suggests that its presence would reinforce the observed intra-receptor interaction through a combination of steric effects and dispersive interactions. In the case of the longer receptor **2** this pathway is not accessible since the bulky groups are beyond interacting distance. This intra-receptor reinforcement has been observed previously to be a key factor in other host–guest systems that have been demonstrated to display cooperative,¹ or non-statistical binding behaviour.^{14,49,50} In other words, as demonstrated by speciation curves in Fig. 9

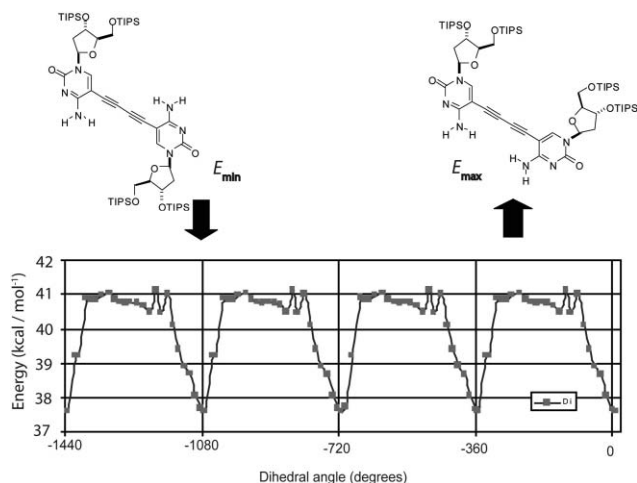


Fig. 16 Torsional energy vs. dihedral angle for dialkyne **2**. E_{\min} centred on 0° and E_{\max} over much of the dihedral rotation.

and Fig. 11, the shorter receptor **1** shows an unexpectedly large stepwise association constant for the binding of a second guanosine molecule, leading to a greater concentration of **1·3·3** than would otherwise be expected.

The assignment of such non-statistical behaviour to a binding event is not straightforward, since classic Scatchard plots ought to be applied only to strictly intermolecular binding events.⁵¹ The system presented here meets this criterion and hence in the case of **1·3** can be described as having reinforced,⁴⁹ or non-statistical binding, more usually described as exhibiting ‘positive cooperativity’. Although such cooperativity has long been recognised in proteins⁵² and macromolecules,^{53,54} self-assembly processes involving small molecules, often referred to as ‘cooperative’, frequently show expected statistical behaviour upon closer analysis. In contrast, the **1·3** pairing investigated here does appear to show non-statistical behaviour. Computational data analysis to further explore these effects in these model systems is ongoing, together with fuller isothermal titration calorimetry data acquisition and interpretation.

Conclusion

The binding of receptors **1** and **2** with **3** has been studied by NMR titration and an improved curve fitting procedure was used to analyze the titration result. Compared to the implementation of several algorithms, a number of advantages are apparent, although the limitations of this classic approach as implemented are also becoming clearer.¹³ The approach herein allows the use of readily available software to treat more complex systems without use of polynomial equations; additionally by allowing the concentration of host to vary over the titration interval the fraction of guest bound in the complex, p , remains with the desired range $0.2 < p < 0.8$ over a wider concentration of guest than would be otherwise possible. There are however issues to be addressed in that: (i) simultaneous fitting of higher equilibria to experimental data presents a more serious programming challenge, especially if errors are to be estimated during that process; (ii) the current approach requires user intervention during the iterations to achieve the best data fit.

The dimerization constants of **1** and **2** were found to be $83 \pm 3 \text{ M}^{-1}$ and $340 \pm 7 \text{ M}^{-1}$ in deuteriochloroform respectively. The self-association of guanosine **3** was described in terms of equilibria between monomer, dimer and tetramer and the association constants were found to be $K_{3,3} = 370 \pm 72$ and $K_{3,3,3,3} = 15 \pm 1 \text{ M}^{-1}$ in deuteriochloroform. All these self-associations were included in the subsequent curve fitting of the NMR titration data of **1** or **2** with **3** although the limitations of the current approach mean that concurrent optimisation of all equilibria is not yet possible. The stepwise association constants for **1** and **3** were found to be $K_{1,3} = 5180 \pm 210$ and $K_{1,3,3} = 4800 \pm 170 \text{ M}^{-1}$, demonstrating non-statistical binding (positive cooperativity). Analogously for **2** stepwise equilibria were $K_{2,3} = 8100 \pm 380$, $K_{2,3,3} = 1170 \pm 80 \text{ M}^{-1}$ respectively, which is close to statistical (non-cooperative) binding. Basic molecular mechanics modelling shows that the mono-alkyne receptor **1** possesses hindered rotation around the central axis that may partly explain the origin of the observed non-statistical binding or positive cooperativity upon interacting with guest **3**. This is notable since there are relatively few examples

of small molecule systems that are now understood to display such behaviour.

Experimental

NMR titrations were carried out in CDCl₃ (Aldrich) used as received and residual CHCl₃ was used as the internal reference $\delta = 7.26$ ppm. A solution of the host **1** or **2** was prepared in 500 μ l of CDCl₃ (0.013 M) in a clean, dry NMR tube. The guest **3** stock solution was similarly prepared in 1.5 ml of CDCl₃ (0.023 M) and titrated into the NMR tube *via* a Hamilton microlitre syringe. Except for the first data point, the concentrations were calculated using the integration of tetramethylsilane as an internal standard. The ¹H NMR spectra were recorded using a Bruker DPX400 spectrometer. The aromatic and N–H signals were monitored as successive aliquots of guest stock solution were added (15 additions up to 1500 μ l).

The NMR titration data were analysed by numerical methods in a Microsoft Excel[®] spreadsheet using the standard 'Solver' feature. The spreadsheets are made available at <http://go.warwick.ac.uk/marshgroup>. The NMRTit program was kindly provided by Professor C. A. Hunter, University of Sheffield, implemented on an Apple Macintosh 7200/90 and the graphical data captured as a screenshot. A detailed description of the curve-fitting method along with the ITC experiment is provided in the ESI.†

Computational experiments

Calculations were carried out on a PC workstation using MOE 2006.08 and the MMFF94x force field as supplied. Solvation effects were treated *via* the reaction field electrostatic term with a solvent dielectric of 10. Dihedral restraints were applied using both *ortho* carbons adjacent to the alkyne bond(s) such that a torsion angle of zero corresponded to *syn* NH₂ groups. Stepped rotations around the alkyne bond(s) were achieved by applying torsional restraints in 15 degree increments for four complete rotations to generate the energy profiles in Fig. 15 and Fig. 16. Any restraint energy was subtracted from the total and the dihedral angle used in the plots corresponds to the average of the actual dihedrals. Two restraints were essential to prevent non-colinearity of the alkyne bonds, particularly for receptor **2**.

Acknowledgements

AL would like to thank the Department of Chemistry, University of Warwick for funding. The authors also thank the reviewers for very useful comments and suggestions and Dr David Fox, University of Warwick, Department of Chemistry for helpful discussions.

References

- 1 J. D. Badjic, A. Nelson, S. J. Cantrill, W. B. Turnbull and J. F. Stoddart, *Acc. Chem. Res.*, 2005, **38**, 723–732.
- 2 G. Ercolani, *J. Phys. Chem. B*, 2003, **107**, 5052–5057.
- 3 A. Marquis, J. P. Kintzinger, R. Graff, P. N. W. Baxter and J. M. Lehn, *Angew. Chem., Int. Ed.*, 2002, **41**, 2760–2764.
- 4 W. P. Jencks, *Proc. Natl. Acad. Sci. U. S. A.*, 1981, **78**, 4046–4050.
- 5 M. I. Page and W. P. Jencks, *Proc. Natl. Acad. Sci. U. S. A.*, 1971, **68**, 1678–1683.
- 6 G. Ercolani, *J. Am. Chem. Soc.*, 2003, **125**, 16097–16103.
- 7 G. Ercolani, *Org. Lett.*, 2005, **7**, 803–805.
- 8 A. D. Hughes and E. V. Anslyn, *Proc. Natl. Acad. Sci. U. S. A.*, 2007, **104**, 6538–6543.
- 9 G. Ercolani, C. Piguat, M. Borkovec and J. Hamacek, *J. Phys. Chem. B*, 2007, **111**, 12195–12203.
- 10 J. L. Sessler, C. M. Lawrence and J. Jayawickramarajah, *Chem. Soc. Rev.*, 2007, **36**, 314–325.
- 11 A. Marsh, N. W. Alcock, W. Errington and R. Sagar, *Tetrahedron*, 2003, **59**, 5595–5601.
- 12 S. Stoncius, E. Orentas, E. Butkus, L. Ohrstrom, O. F. Wendt and K. Wärnmark, *J. Am. Chem. Soc.*, 2006, **128**, 8272–8285.
- 13 F. G. J. Odille, S. Jönsson, S. Stjernqvist, T. Rydén and K. Wärnmark, *Chem.–Eur. J.*, 2007, **13**, 9617–9636.
- 14 K. A. Connors, *Binding Constants. The Measurement of Molecular Complex Stability*, Wiley, Chichester, 1987.
- 15 L. Fielding, *Tetrahedron*, 2000, **56**, 6151–6170.
- 16 K. Hirose, *J. Inclusion Phenom. Macrocyclic Chem.*, 2001, **39**, 193–209.
- 17 C. S. Wilcox, in *Frontiers in Supramolecular Organic Chemistry and Photochemistry*, ed. H.-J. Schneider, H. Durr and J.-M. Lehn, VCH, Weinheim, 1991.
- 18 H.-J. Schneider, and A. K. Yatsimirsky, *Principles and Methods in Supramolecular Chemistry*, Wiley, Chichester, 1st edn, 2000.
- 19 M. Saunders and J. B. Hyne, *J. Chem. Phys.*, 1958, **29**, 1319–1323.
- 20 S. C. Zimmerman and B. F. Duerr, *J. Org. Chem.*, 1992, **57**, 2215–2217.
- 21 SpecFit, <http://www.bio-logic.info/rapid-kinetics/software.html>, accessed 7 November, 2008.
- 22 C. Frassinetti, S. Ghelli, P. Gans, A. Sabatini, M. S. Moruzzi and A. Vacca, *Anal. Biochem.*, 1995, **231**, 374–382.
- 23 P. Kuzmic, *Anal. Biochem.*, 1996, **237**, 260–273.
- 24 Prism, <http://www.graphpad.com/prism/prism.htm>, accessed 7 November, 2008.
- 25 M. J. Hynes, *J. Chem. Soc., Dalton Trans.*, 1993, 311–312.
- 26 C. Frassinetti, L. Alderighi, P. Gans, A. Sabatini, A. Vacca and S. Ghelli, *Anal. Bioanal. Chem.*, 2003, **376**, 1041–1052.
- 27 A. P. Bisson, C. A. Hunter, J. C. Morales and K. Young, *Chem.–Eur. J.*, 1998, **4**, 845–851.
- 28 M. D. Cowart, I. Sucholeiki, R. R. Bukownik and C. S. Wilcox, *J. Am. Chem. Soc.*, 1988, **110**, 6204–6210.
- 29 V. G. H. Lafitte, A. E. Aliev, P. N. Horton, M. B. Hursthouse and H. C. Hailes, *Chem. Commun.*, 2006, 2173–2175.
- 30 J. P. Clare, A. J. Ayling, J. B. Joos, A. L. Sisson, G. Magro, M. N. Perez-Payan, T. N. Lambert, R. Shukla, B. D. Smith and A. P. Davis, *J. Am. Chem. Soc.*, 2005, **127**, 10739–10746.
- 31 H. Dodziuk, K. S. Nowinski, W. Kozminski and G. Dolgonos, *Org. Biomol. Chem.*, 2003, **1**, 581–584.
- 32 G. Pistolis and A. Malliaris, *Chem. Phys. Lett.*, 1999, **310**, 501–507.
- 33 G. Pistolis and A. Malliaris, *Chem. Phys. Lett.*, 1999, **303**, 334–340.
- 34 L. D. Williams, N. G. Williams and B. R. Shaw, *J. Am. Chem. Soc.*, 1990, **112**, 829–833.
- 35 J. Sartorius and H. J. Schneider, *Chem.–Eur. J.*, 1996, **2**, 1446–1452.
- 36 D. C. Harris, *J. Chem. Educ.*, 1998, **75**, 119–121.
- 37 S. Walsh and D. Diamond, *Talanta*, 1995, **42**, 561–572.
- 38 R. B. Martin, *Chem. Rev.*, 1996, **96**, 3043–3064.
- 39 L. D. Williams, B. Chawla and B. R. Shaw, *Biopolymers*, 1987, **26**, 591–603.
- 40 G. Gottarelli, S. Masiero, E. Mezzina, G. P. Spada, P. Mariani and M. Recanatini, *Helv. Chim. Acta*, 1998, **81**, 2078–2092.
- 41 G. Gottarelli, S. Masiero, E. Mezzina, S. Pieraccini, J. P. Rabe, P. Samori and G. P. Spada, *Chem.–Eur. J.*, 2000, **6**, 3242–3248.
- 42 T. Giorgi, F. Grepioni, I. Manet, P. Mariani, S. Masiero, E. Mezzina, S. Pieraccini, L. Saturni, G. P. Spada and G. Gottarelli, *Chem.–Eur. J.*, 2002, **8**, 2143–2152.
- 43 M. C. Masiker, C. L. Mayne and E. M. Eyring, *Magn. Reson. Chem.*, 2006, **44**, 220–229.
- 44 C. Nativi, M. Cacciarini, O. Francesconi, A. Vacca, G. Moneti, A. Ienco and S. Roelens, *J. Am. Chem. Soc.*, 2007, **129**, 4377–4385.
- 45 C. S. Wilcox, J. J. C. Adrian, T. H. Webb and F. J. Zawacki, *J. Am. Chem. Soc.*, 1992, **114**, 10189–10197.
- 46 A. Vacca, C. Nativi, M. Cacciarini, R. Pergoli and S. Roelens, *J. Am. Chem. Soc.*, 2004, **126**, 16456–16465.

-
- 47 S. C. Zimmerman, P. S. Corbin and B. Xie, *Struct. Bonding*, 2000, **96**, 63–94.
- 48 MOE2006.08, *Chemical Computing Group, Montreal*, 2006.
- 49 Z. Rodriguez-Docampo, S. I. Pascu, S. Kubik and S. Otto, *J. Am. Chem. Soc.*, 2006, **128**, 11206–11210.
- 50 S. Otto, *Dalton Trans.*, 2006, 2861–2864.
- 51 J. Hamacek and C. Piguet, *J. Phys. Chem. B*, 2006, **110**, 7783–7792.
- 52 A. Horovitz and A. R. Fersht, *J. Mol. Biol.*, 1990, **214**, 613–617.
- 53 J. Wyman and S. J. Gill, *Binding and linkage: functional chemistry of biological macromolecules*, University Science Books, Mill Valley, California, US, 1990.
- 54 E. Di Cera, *Thermodynamic theory of site-specific binding processes in biological macromolecules*, Cambridge University Press, Cambridge, 1995.